

Modeling Lipid Release from Almond Seeds in the Digestive Environment

Spring 2017 EBS270 Project

Clay Swackhamer

Alex Olenskyj

Ke Wang

Introduction

A nutrient that enters the body in the form of a food item with some physical structure is not immediately absorbed by the body. Before it can be taken up by intestinal cells and enter the bloodstream, the nutrient must first exit the food matrix where it is contained¹. The proportion of the nutrient that can be released from the food matrix, which is defined as its bioaccessibility², limits the total amount of nutrient that can be further digested and potentially absorbed by the body. The mechanisms of regulating the bioaccessibility of nutrients from food are not fully understood^{2,3}. In this project, fractured almond seeds in the digestive environment were used as a model system. Lipids are the dominant nutrient in almonds by total caloric contribution², and thus the bioaccessibility of lipid is an important factor in determining the metabolizable energy of almonds.

The ability to predict the bioaccessibility of nutrients from almonds based on their physical properties is critical to enabling design of functional foods containing almonds⁴, such as products to maximize satiety. In addition, some consumers have specific needs for foods which lead to a predictable state of postprandial lipemia, due to conditions such as cardiovascular disease⁵⁻⁷ or diabetic-linked hyperlipidemia⁸. Furthermore, almonds are an agricultural product of interest in California, with production of 1.81 billion pounds in 2015, total economic footprint of \$21.5 billion, and contribution of 104,000 jobs to the state's economy⁹.

Literature Review

The almond seed, also called the kernel, is the edible part of the almond fruit. The almond seed is composed of an embryo, which is surrounded by a skin, called the testa. The pericarp, which encloses the kernel, contains a green fleshy hull and a hard, pitted shell². The almond cotyledon is a white, lipid bearing tissue, which is made up of approximately spherical cells, called parenchymal cells, each with a relatively thin, yet chemically resistant cell wall with thickness of approximately 0.1 μm to 0.3 μm ¹⁰. These cellular structures were investigated by Grassby, et. al³ using microscopy. Some of their results are shown in Figure 1.

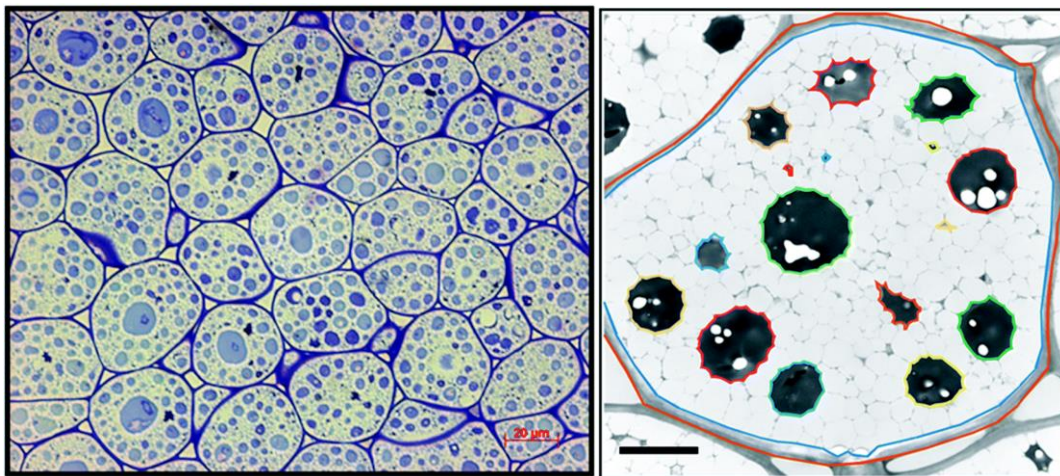


*Figure 1: **Left:** Light microscopy image of parenchyma cells in almond tissue. Lipid bodies are clear, while intracellular components and cell walls are stained blue. **Right:** Transmission electron microscopy image of single almond parenchyma cell. Lipid bodies are white, and protein inclusions are dark. Images are from Grassby, et. al. 2014, "Modelling of nutrient bioaccessibility in almond seeds based on the fracture properties of their cell walls." *Food and Function*. 5. 3096-3106.*

The amount of lipid contained in whole natural almonds ranges from 44 to 61 grams per 100g of almond¹¹, depending on the harvest and variety¹². Almond seeds can be eaten in various forms, and varying shapes and sizes of almond particles can be obtained through processing the whole natural, blanched, and roasted seeds.

For the purposes of this project, it is important to distinguish between almond particles and almond cells. Almond particles are fragments of whole almonds, and are comprised of numerous cells. Almond particles vary widely in size depending on how the almond seed is processed, with a with a general range from $< 250 \mu\text{m}$ (finely ground almond flour) to $2000 \mu\text{m}$ (masticated almonds)². Almond cells are the individual cells of the almond parenchyma, which are roughly spherical, $36\mu\text{m}$ in diameter, and protected by a cell wall³. Several studies have reported that lipid released from almonds during digestion is higher from almond foods made up of smaller particles¹³⁻¹⁶. It is hypothesized that this increased lipid bioaccessibility is due to increased fractured or exposed surface cells relative to the total number of cells in the meal².

After consumption, almond fragments are processed by the stomach. This is called the gastric phase of digestion. During gastric digestion, almond particles are subjected to immersion in an enzyme rich, acidic solution that has pH of roughly 1.5 to 3.0^{17,18}. This is visualized in Figure 2.

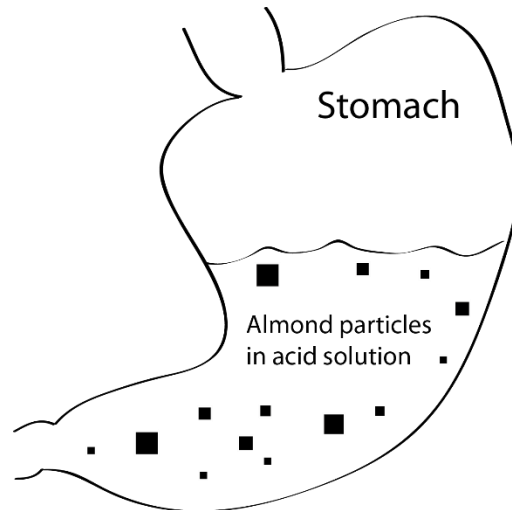


Figure 2: Gastric digestion of almond particles occurs in the stomach

Lipid release in the stomach and the remainder of the gastrointestinal tract from cells contained within the particles with intact cell walls is minimal. This is hypothesized to be due to encapsulation of the lipid contents by an intact cell wall, which prevents penetration of enzymes such as lipases, thus hindering the rate and extent of nutrient release^{10,15,19,20}. However, lipid can be released from cells which are ruptured during mastication, or that have a cell wall which becomes breached during the course of digestion^{13,15,16,19,20}.

Therefore, when a certain amount of almond is reduced into smaller particles (e.g. almond slices, cubes, or powder), more cells on the surface of particles become exposed relative to the total number of cells in the sample. These cells on the outer surface are likely ruptured during size reduction and lipid within them can be rapidly released and become bioaccessible³. It has been demonstrated by previous researchers that overall lipid release from an almond meal is dominated by contributions from cells ruptured during a fracture or mastication event^{19,21}. However, microscopy experiments on both *in vivo* and *in vitro* digested almonds have demonstrated that lipid is released from several layers of the almond, starting with the exterior layer and progressing to as many as five layers depth over the course of a 12-hour digestion (Figure 3)^{20,21}. Also, experimental results show that models which only consider the initial surface area of particles as able to contribute lipid tend to under-predict the overall lipid release from the almond meal¹⁰.

An initial hypothesis for this phenomenon was that lipase diffusion through cell wall pores allowed for the breakup of internal lipid bodies, and subsequent release of free fatty acids through the same pores in the cell wall¹⁰. The radius of gyration of gastric and pancreatic lipases (50kDa) are roughly 1.7 and 1.9 nm, respectively^{22,23}. This is below the pore size of cell walls¹⁰.

However, *in vitro* digestion experiments on almonds in the presence of fluorescent labelled lipases showed no evidence of diffusion through intact cell walls, casting doubt on the hypothesized mechanism¹⁰. An alternative hypothesis is proposed in this project, which is that lipid release from cells on interior layers is due to the breaching or weakening of their cell walls due to diffusion of acid into the particle. Following this disruption of the cell walls, the lipid contained within the cells becomes accessible to enzymatic action and capable of releasing from the almond matrix.

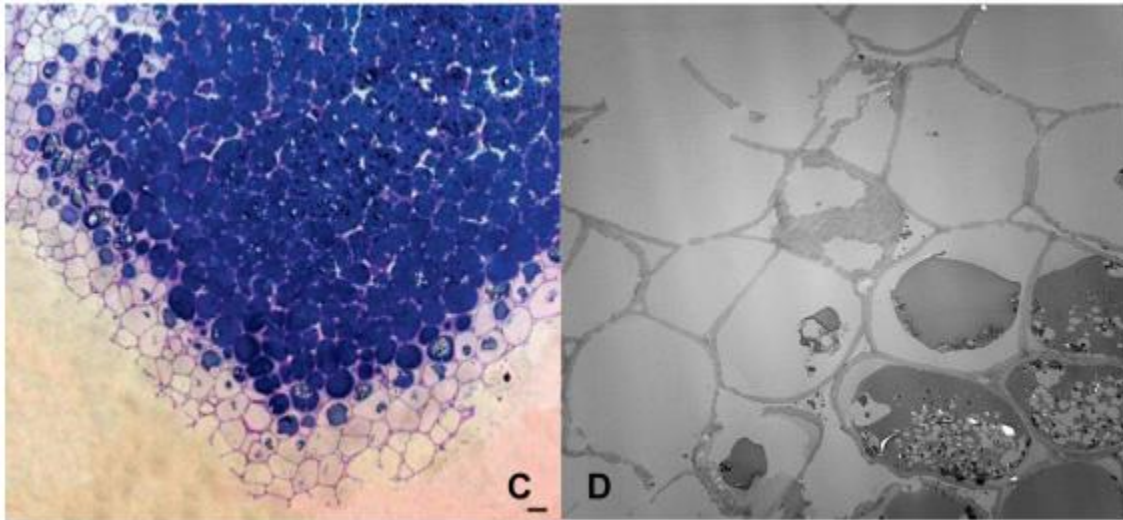


Figure 3. The intact cells with intracellular nutrients were stained with toluidine blue. Light microscopy section after 12 h in vivo digestion (C) showed some breached and intact cells, at and beneath the surface of a 2-mm natural almond cube, had lost the stained materials, indicating the release of nutrient underneath the surface (about 3 to 5 layers) of the almond cube and transmission electron microscopy after 12 h in vivo digestion (D) confirmed the losses of intracellular contents from intact cells underneath the surface (adapted from Mandalari et al., 2008)

Acids are present in gastric digestion and are capable of hydrolyzing biological molecules such as cellulose and other structural carbohydrates^{20,24} that are known components of the almond cell wall¹². Under this hypothesis, the rate of release of lipid from almonds is still expected to increase as initial surface area of particles increases. However, the surface area that is available for lipid release from a given almond particle is expected to increase as digestion elapses, due to the penetration of acid into the particle. As the acid front meets progressively more layers of cells, the lipids contained in the damaged cells are expected to become bioavailable. This is visualized in figure 4.

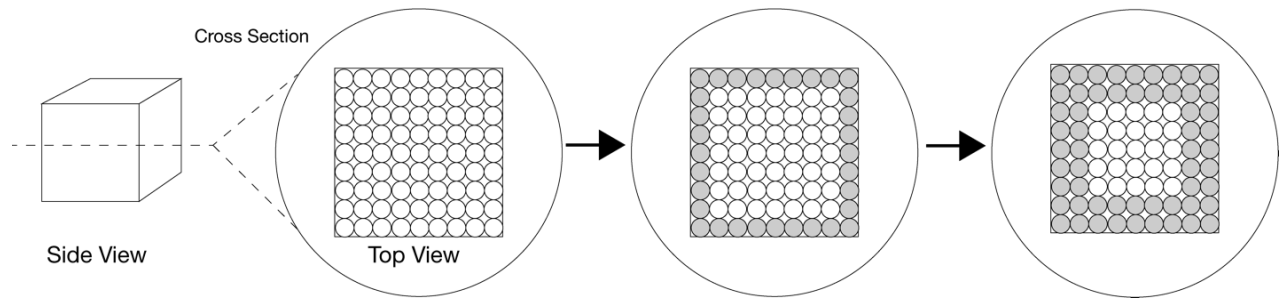


Figure 4: Lipid release from successive layers during gastric digestion in a 3D cubic model of an almond particle

The overall goal of the model is to predict lipid release based on the properties of the almond meal, such as particle size distribution. This is because lipid release is of interest to the medical and nutritional communities for optimizing foods for consumer health. Particle size of almond foods is the main independent variable. This is because lipid release from almonds has been shown to be dependent on particle size, and the theory of cell wall encapsulation of lipid bodies provides a framework in accordance with clinical results. This framework can be used to create a geometrical model, as shown in this project. Such a model could then be tested through actual experiments. To this end, using particle size as the main predictive variable provides another benefit, which is that it can be measured in a laboratory, and when coupled with *in vitro* digestive experiments, does not require invasive measurements of gastric conditions or expensive clinical collection of gastric contents or feces.

Existing models are available for predicting the lipid release from almond particles based only on particle size (assuming that particles are monodisperse, have constant size, have cubical geometry, and that almond cells are identical spheres of constant diameter)³. One such model will be derived in a future section. However, no previous work has considered a model for acid penetration into almond particles. To construct a model for lipid release from almond particles that accounts for interior layers of cells hydrolyzed by acids, some engineering assumptions must be developed.

Engineering Assumptions:

1. **Lumped Nutrient:** An initial assumption in this model is that all the lipid in an almond can be considered as a single nutrient. In reality, almonds contain oleic, linoleic, palmitic, stearic, and palmitoleic acid, but oleic and linoleic acids account for roughly 90% of the total lipid¹². It is expected that these lipids will behave the same way, at least for the purposes of the model. That is, they are expected to exit parenchymal cells when the cell wall has been breached, and otherwise remain inside the cell.
2. **Constant almond cell diameter:** Almond cells are identical spheres of diameter 36 μm . This assumption is based on microscopy experiments on almond parenchyma tissue, which were used by previous researchers to determine that almond cells had a consistent size and geometry^{3,20}. A sub-assumption is that these spherical cells do not change in size or geometry during digestion.
3. **Cubical almond particles:** In order to develop a framework consistent with previous theoretical models³ and experimental data²⁰, it is assumed that almond particles are cubical. These almond particles are the result of chewing, grinding, or otherwise fracturing of whole natural almonds.
4. **Homogeneous and isotropic cell wall:** For the purposes of this model, it is also assumed that almond cell walls are comprised of homogeneous and isotropic material.
5. **Cell wall thickness is constant** for all cells in the almond. This enables the modeling of acid diffusion into the cell using in one dimension.
6. **Constant bulk solution:** Also, it is assumed that the pH in the bulk solution is constant and equal to 1.8 (acid concentration of constant $10^{-1.8}$ M).
7. **No lipid can be released from intact cells.** However, the lipid contents of breached cells are released instantaneously. In physical terms, this means that the diffusion of lipid through the cell itself is negligible, and degradation of the almond cell wall is the rate limiting step in overall lipid release.
8. **Lone particles:** It is assumed that particles in digestion are not affected by other particles. Thus, no treatment effect of agglomeration, grinding, shielding, or buffering capacity is considered.
9. **Convection of acid is not rate limiting:** It is assumed that the concentration of acid at the surface of a particle is equal to the concentration of acid in the bulk solution. This means that the convection of acid around the particles is much greater than the diffusivity of acid into the particles.

10. **Diffusion follows Fick's Law of Diffusion.** Although in a future work, the almond cell wall may be considered as a porous medium, this study will assume that the almond cell walls are non-porous solids.
11. **Diffusion can be modelled in one dimension across a single cube face.** In physical terms, it is assumed that diffusion through edges and corners of cubes is no faster than diffusion through a face of the cube. Consequently, cells are exposed layer-by-layer, with each cell in a given layer being breached by acid simultaneously.
12. **Diffusion through cell wall is rate limiting:** It is assumed that the time required for acid to diffuse through the interior of cells is negligible compared to the time required for acid to diffuse through the cell wall.
13. **Cell wall rupture occurs at a H^+ concentration of 10^{-3} M (pH 3):** Once the entire cell wall thickness on one side of the intact cell has come to a pH of 3, the cell is assumed to rupture.
14. **Almonds naturally have a pH of 7.**

Modeling acid diffusion into almond matrix

A model of lipid bioaccessibility from an almond meal must consider not only the lipid contribution from cells which are initially on the surface of almond particles, but also the contribution from cells which are “revealed” as acid diffuses into the interior of the particles, breaching the cell walls of outer layers of cells and enabling their lipids to be released. Consideration of this effect requires a physical model for diffusion of acid into the almond particle. This rate of diffusion can be represented in one dimension by the simple time-dependent diffusion equation (Fick’s Second Law).

$$\frac{\partial C}{\partial t} = D \frac{\partial^2 C}{\partial x^2}$$

Where C represents the concentration of acid, t represents time, and x represents the distance through cell walls which the acid travels.

This is a well-known equation; however, the x -term should be explained. The x -term represents the amount of cell wall material that the acid must penetrate.

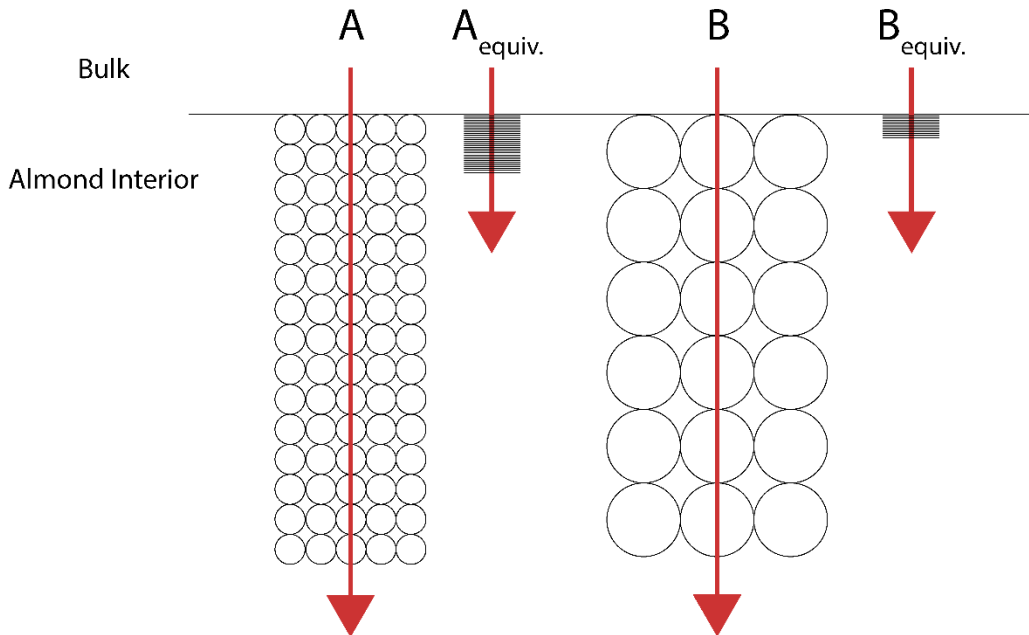


Figure 5: Demonstration of the need to monitor acid diffusion based on the distance the acid travels through cell wall material. In system A, the equivalent amount of cell wall material that must be diffused through is represented as $A_{equiv.}$ System B is displayed likewise. Although the cell size is assumed to be uniform and unchanging in this study, consideration of only cell wall material eliminates the need to monitor cell size throughout the digestion.

In the image above, acid will take longer to diffuse through path A than it will to diffuse through path B. In order to correct for this, x will not represent the length in space, and will instead represent the thickness of cell wall material that the acid must penetrate.

This can be thought of as a local coordinate system, where the 1-D side length of the cube in physical space is mapped to the x dimension. As the middle of the cube, x is zero. The edge of the cube is $s/2$ millimeters away from the center in physical space, therefore $x(s/2)$ will represent the edge of the cube in “cell wall space”.

The boundary conditions for this partial differential equation will be as follows:

$$\frac{\partial C}{\partial x} = 0 \text{ at } x = 0$$

to represent the symmetry across a cube, and:

$$C\left(x\left(\frac{s}{2}\right), t\right) = C_{Bulk} = 10^{-1.8}$$

to represent the concentration on the cube surface being equal to the bulk concentration of the stomach (diffusion is rate-limiting). Finally, the initial condition is

$$C(x, 0) = 10^{-7}$$

representing an initial concentration of H^+ equal to that of pH 7.

Solving this equation would give a concentration profile in time and space. To couple this equation to lipid release, a threshold concentration must be established above which the cell wall will be considered hydrolyzed.

This threshold could likely be found with experimentation; however, in this model it will be approximated as occurring at a pH of 3. Therefore, the distance at which the pH of the cell wall material has reached 3 can be mapped over time. Once the “front” of pH 3 is identified, there are two ways to couple the diffusion with the lysing of cells. The simpler way is to determine the amount of time necessary to reach pH 3 at $x = \theta$, where θ represents the thickness of one cell wall. The total digestion time can be divided by this time value to obtain the number of cell walls lysed by the acid:

$$q(t) = \left\lfloor \frac{t}{t_\theta} \right\rfloor$$

where q represents the number of layers which have been ruptured, and t_θ represents the time required to breach a single cell wall. Due to the floor brackets shown above, q will always be a

whole number, and the plot of q over time will appear stepwise. This is because it is assumed that the layers of cells on the outside of an almond particle break down sequentially, layer-by-layer.

The value of D , the diffusivity of acid in the almond matrix, is not known explicitly. However, Mandalari et al. showed in 2008 that lipid is released from 3-5 layers of almond cells in 12 hours⁶. Assuming the first cell is ruptured by the initial size-reduction process, this constitutes 8 cell walls breached by acid for 5 layers of penetration (4 additional layers underneath the outer layer, which is assumed to be ruptured at the start of digestion). The PDEPE function in MATLAB can be used to determine the value of D from that information by using the function inside of a DO or FOR loop starting with a small D value, and incrementally increasing the D value until the value is such that a pH of 3 is reached at a location equivalent to 5 layers into the almond matrix within 12 hours. In this analysis, a pH of 3 can be targeted at a location equivalent to one cell wall thickness equivalent within 12/8 hours (1.5 hours).

The above analysis relies heavily on the assumption that once the cell wall is breached by acid, the pH in the newly exposed cell quickly equilibrates with the bulk pH. This assumption can be relaxed; however, this would require a modification of the initial differential equation. The value of diffusivity of acid in cell wall material can be made to be dependent on the concentration of acid:

$$D = f(C)$$

such that diffusivity increases with concentration of acid. This is because cell wall material which has been degraded by acid is predicted to allow faster penetration of acid. The following relationship is proposed:

$$D = \frac{-A}{\log(C)}$$

Where D is diffusivity, C is concentration of acid in molarity, and A is a parameter. This equation can be thought of as a linear approximation with respect to pH.

If this method were to be used, the original equation will be modified as such:

$$\frac{\partial C}{\partial t} = \frac{-A}{\log(C)} \frac{\partial^2 C}{\partial x^2}$$

Where again, C represents concentration, A is a diffusivity parameter, t represents time, and x represents the distance through cell walls which the acid travels.

Just like in the simpler analysis considering only the time required to breach one cell wall, the concentration-dependent diffusion analysis can also utilize the literature result from Mandalari et al.⁶ since only the A parameter needs to be determined. For this optimization, a DO or FOR loop can be used once again with the target of 8 cell wall thickness equivalents in 12 hours of exposure to acid to determine the proper value of A . This method was chosen to explore further in the model proposed in this report.

In summary, modeling acid diffusion into the almond particle allows for the calculation of the number of cell layers in an almond particle that will be exposed at some point during gastric digestion, and thus will be able to release lipid contents. This number will always be greater than the number of cells initially on the outermost layer of the cubical particle, as additional cells are revealed by acid hydrolysis of the cell walls of cells on the outer layers, progressively revealing cells on interior layers.

The parameter q can also represent the number of layers that release lipid in the more complex diffusion model.

$$q(t) = \left\lfloor \frac{x(t|_{c=10^{-3}})}{2\theta} \right\rfloor$$

Where $q(t)$ represents the number of breached layers of cells at time t , t represents the elapsed time the particle is in the gastric environment, θ represents the thickness of one cell wall, and $x(t|_{c=10^{-3}})$ denotes the total distance where concentration is equal to 10^{-3} over time. The denominator is 2θ because two cell walls need to be ruptured in order to release the contents of one layer.

This model represents acid diffusion, however it does not allow for calculation of an overall amount of lipid release without further modeling. Since the original goal of the model was to predict overall lipid release from almond particles, a model must be found that can accomplish this, in accordance with the assumptions of cubical particles, complete lipid release from breached cells, and zero lipid release from interior cells with intact cell walls.

A suitable model framework was found in the work conducted by Grassby, et. al (2014), who derived an expression for the number of cells on the surface of a cubical particle. This was then expressed as a percentage of the total number of cells in the cubical particle, which is the same as the percentage of lipid released during digestion, given the assumptions of complete release from surface cells and zero release from interior cells, along with a uniform lipid concentration and cell size. However, the original model did not consider the effect of acid diffusion into the particle, which is predicted to reveal additional layers of cells as time progresses. This is the contribution of the current project, and in a future section it will be shown how this can be integrated into the original Grassby model. However, before this step can be shown, a few early steps in the development of the original model must be shown. For the derivation of the original model without the improvements developed in the current project, please see Appendix A.

Integration with Grassby model

In this section, the derivation will be conducted for a model developed by Grassby et al³ to predict the lipid release from an almond particle as a function of particle size. Then, the consideration of acid diffusion will be made by integrating the work from the previous section into the Grassby model.

As in the above section, Grassby, et. al. considered the masticated almond to consist of identical, cubical particles, and assumed that all lipid from a cell on the boundary of the cube is released during digestion, and no lipid from cells in the interior of the cube is released. This assumption was the same as was made in the “model assumptions” section above. It is visualized in Figure 6.

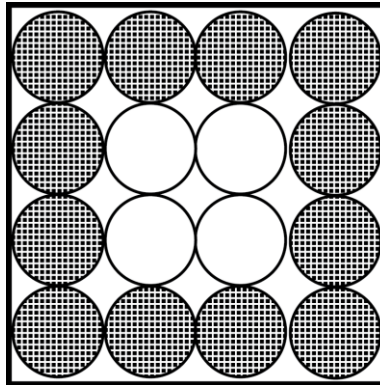


Figure 6: Cross section of a cube of almond comprised of spherical cells. Patterned cells are on the boundary and are assumed to release all of their lipid contents. White cells are part of the interior and are assumed to release none of their lipid contents.

The cubical geometry was assumed not for the purposes of accurate approximation of the true distribution of almond particle shapes after mastication, but for ease of developing a formula for the number of cells on the outer surface. An example almond particle is shown in Figure 7.

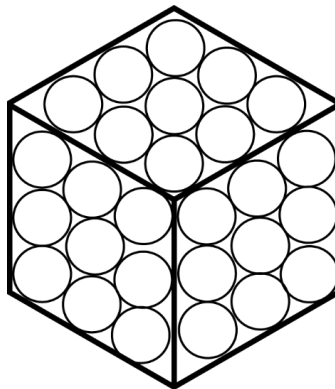


Figure 7: Representation of a cubical almond particle comprised of spherical cells. In this view, all the illustrated cells reside on an exposed surface and are therefore assumed to completely release their lipid contents.

Next, the average number of cells in an almond cube was expressed as the ratio of the volume of an almond cube to the volume of an idealized spherical almond cell, multiplied by the packing

density of spherical cells into the cube.

$$\langle N_{total} \rangle = \frac{V_{cube}}{V_{cell}} * P$$

$$\langle N_{total} \rangle = \frac{s^3}{\frac{4}{3}\pi\left(\frac{d}{2}\right)^3} P$$

Where:

$\langle N_{total} \rangle$ = average number of cells in the cube

s^3 = side length of a cube (μm^3)

d = diameter of an almond cell (μm)

P = packing density of almond cells into the cube

A packing density $P=1$ would mean that all space in the cube is occupied by one cell. This is the same as assuming that there is no intracellular space. However, it is important to point that no numerical value was assumed for the packing density P , as it was cancelled out of the equations in a later step (when the number of surface cells was expressed as a ratio of the total number of cells in the cube).

With the previous equations developed, the total number of exposed cells on a cube of almond tissue was expressed as the sum of the number of exposed cells on each individual face of the cube

$$\langle N_{exposed} \rangle = n_1 + n_2 + n_3 + n_4 + n_5 + n_6$$

Where:

$\langle N_{exposed} \rangle$ = number of exposed cells on an entire cube of almond tissue

$n_1 \dots n_6$ = number of exposed cells on each surface of the cube 1-6

Next, the number of exposed cells on a face of the cube was expressed as an area fraction: the area of the face of the cube divided by the area of an idealized spherical cell, but expressed in 2D:

$$n_1 = \dots = n_6 = \frac{s^2}{Area_{cell}} * P$$

Where:

$n_1 \dots n_6$ = number of exposed cells on each surface of the cube 1-6

s^2 = area of a face of the cube (μm^2)

$Area_{cell}$ = area of a cell with 2D profile diameter d'

P = packing density of almond cells into the cube

Grassby, et. al. used the profile diameter of a cell (d') instead of its real diameter (d), as cell diameters were measured using light microscopy, which was a two-dimensional approximation.

This is because light microscopy is used to measure the area of planar slices of cells, which are actually three-dimensional spheres. The profile diameter was converted to the real diameter using the following expression:

$$d = \frac{4}{\pi} d'$$

Where:

d = real diameter of a cell

d' = two-dimensional measured diameter (profile diameter) of the cell

The linear conversion between profile diameter and real cell diameter was developed by Weibel. The area of a cell with two-dimensional profile diameter d' was thus:

$$Area_{cell} = \frac{\pi}{4} d'^2$$

Where:

d' = profile diameter of cell (as measured by light microscopy) = $\frac{\pi}{4} d$

$$Area_{cell} = \frac{\pi}{4} \left(\frac{\pi}{4} d \right)^2$$

$$Area_{cell} = \frac{\pi}{4} \left(\frac{\pi^2 d^2}{16} \right)$$

$$Area_{cell} = \frac{\pi^3 d^2}{64}$$

Returning to the equation for the number of exposed cells on a given face of the cube:

$$n_1 = \dots = n_6 = \frac{s^2}{Area_{cell}} * P$$

$$n_1 = \dots = n_6 = \frac{\frac{s^2}{\pi^3 d^2}}{64} * P$$

$$n_1 = \dots = n_6 = \frac{64s^2}{\pi^3 d^2} * P$$

This expression for the number of exposed cells on a given face of the cube does not account for additional cells exposed as outer cells are breached by acid that diffuses into the particle. This is considered by integrating the results from the section “Modeling acid diffusion,” where an expression was developed for the number of layers that have been breached, as a function of time.

$$q(t) = \left\lfloor \frac{x(t)}{2\theta} \right\rfloor$$

Where:

$q(t)$ = number of breached layers of cells at time t

t = elapsed time the particle is in gastric environment

$x(t)$ = total distance of acid penetration through cell wall material at time t

θ = thickness of one cell wall

Each layer of cells has depth equal to the diameter of a single cell. Thus, the number of exposed cells on a given face (accounting for additional cells revealed by acid diffusion) is:

$$Cells_{face} = Cells_{outer} + Cells_{layer1} + Cells_{layer2} + \dots + Cells_{layerN}$$

Where:

N = number of layers breached during gastric digestion

$Cells_{face}$ = Total cells revealed on a given cube face

As an example, the total number of cells revealed on a single face of a cube of size s , for breakage of three layers, is shown:

$$Cells_{face} = \frac{64s^2}{\pi^3 d^2} * P + \frac{64s'^2}{\pi^3 d^2} * P + \frac{64s''^2}{\pi^3 d^2} * P$$

Where:

s = original cube size (side length)

s' = size of first layer

s'' = size of second layer

d = cell diameter

In this expression, the sizes refer to the side length of each exposed layer. This can also be formulated in terms of the size of the original face, s , and the diameter of the cells, d :

$$Cells_{face} = \frac{64s^2}{\pi^3 d^2} * P + \frac{64(s - 2d)^2}{\pi^3 d^2} * P + \frac{64(s - 4d)^2}{\pi^3 d^2} * P$$

This can be generalized to any number of breached layers using the following expression:

$$Cells_{face} = \frac{64 \sum_{q=0}^Q (s - 2qd)^2}{\pi^3 d^2} * P$$

Where:

q = number of breached layers

In the above statement, the number of breached layers, q , is zero if the outer surface is the only surface from which cells can release lipid. If the outer layer has been breached, then q is equal to one, and a total of two layers of cells can contribute to lipid release. At time zero, the only

exposed cells are those initially on the outer surface. Thus $q(0)$ is zero, and the expression reduces to the same result that was derived by Grassby: $n_1 = \dots = n_6 = \frac{64s^2}{\pi^3 d^2} * P$

Next, the total number of cells belonging to a given cubical particle that are exposed over the entire course of digestion expressed as the sum of the number of cells that become exposed on all six faces. Assuming that all faces experience acid diffusion and allow for lipid release from breached layers in the same way, the total number of lipid-contributing cells from the cube is six times the number on a single face:

$$\langle N_{exposed} \rangle = 6 * \frac{64 \sum_{q=0}^Q (s - 2qd)^2}{\pi^3 d^2} * P$$

$$\langle N_{exposed} \rangle = \frac{384 \sum_{q=0}^Q (s - 2qd)^2}{\pi^3 d^2} * P$$

Since it was assumed that only the exposed cells released lipid during digestion, the overall percentage of lipid released can be expressed as the ratio of the number of exposed cells to the total number of cells in the cube.

$$Lipid\ release\ (\%) = \frac{\langle N_{exposed} \rangle}{\langle N_{total} \rangle} * 100\%$$

Where:

$\langle N_{exposed} \rangle$ = number of exposed cells on a cube

$\langle N_{total} \rangle$ = total number of cells in the cube, defined previously

$$Lipid\ release\ (\%) = \frac{\left(\frac{384 \sum_{q=0}^Q (s - 2qd)^2}{\pi^3 d^2} * P \right)}{\left(\frac{s^3}{\frac{4}{3} \pi \left(\frac{d}{2} \right)^3} * P \right)} * 100\%$$

$$Lipid\ release\ (\%) = \frac{64d}{\pi^2 s^3} \sum_{q=0}^Q (s - 2qd)^2 * 100\%$$

Finally, the ratio is divided by two, due to the fact that cells fractured in a breakage event (resulting in the formation of the idealized cubes) should not be counted twice.

Thus, the final equation is stated:

$$STM: \text{Lipid release (\%)} = \frac{32d}{\pi^2 s^3} \sum_{q=0}^Q (s - 2qd)^2 * 100\%$$

Dividing by two introduces another assumption, which is that all cells on the surface of an almond particle are fractured. This is considered a reasonable assumption for the case where almonds are consumed with the skin intact, as almond skin is recalcitrant to degradation by enzymes and acids in the human digestive system¹³. This assumption is best understood with an illustration of the idealized fracture event that resulted in two cubes, which is shown in Figure 8.

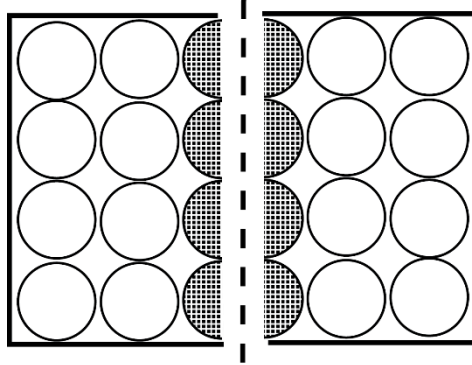


Figure 8: Almond fracture event that results in two cubes.

In this case, it is assumed that only the ruptured cells on a fractured surface are able to release lipid (shaded). The final statement of the STM includes a divisor of two to prevent counting the lipid contribution of the cells on the fracture plane as members of both of the children particles.

This results in a model for the percentage of lipid release from a single almond cube of size s , comprised of identical cells of diameter d . An interesting consequence of expressing the lipid release from the cube in terms of the percentage of total lipid in the cube instead of in absolute terms is that the packing density of the spherical cells in the cube cancels out. Also, if it is assumed that the masticated almond fractures into an ensemble of identical cubes, the percentage of lipid release from one cube is the same as the percentage of lipid released from all of the cubes.

However, an assumption of the above model was that the total number of exposed cells on the cube was equal to six times the number of exposed cells on a single face. There is a problem with this assumption, which is that there are some cells which are shared by more than one face. Cells on the edges of the cube (shared by two adjacent faces) are counted twice. Cells on the corners (where three faces intersect) are counted three times. This means that the above model will always overestimate the lipid release, by counting some exposed cells more than once. This simple model was named the Simple Theoretical Model (STM) by Grassby, et. al, although in the original formulation there was no consideration of a contribution from cells on layers beneath the outer surface due to acid diffusion. That was an original contribution of this project.

However, Grassby, et. al. (2014) did offer an improvement to the STM by deriving a model based on the same assumptions, but that prevented cells from being counted more than once. This was done by defining the number of exposed cells on two opposite faces of the cube (called faces 1 and 2). Since these faces are assumed to share no cells with each other, the number of exposed cells on them is expressed in the same way as it was in the development of the STM:

$$n_1 = n_2 = \frac{64 \sum_{q=0}^Q (s-2qd)^2}{\pi^3 d^2} * P$$

Next, the number of exposed cells on two more faces are defined. These faces share cells on two sides with the previously defined faces, n_1 and n_2 . Thus, they have slightly less cells, as shown in the following formula:

$$n_3 = n_4 = \left(n_1 - 2 * P \left[\frac{\sum_{q=0}^Q (s-2qd)^2}{\frac{\pi}{4} d} \right] \right)$$

Finally, the number of cells on the final faces, n_5 and n_6 , were defined. These faces share cells on all four sides with previously defined faces, n_{1-4} .

$$n_5 = n_6 = \left(n_1 - 4 * P \left[\frac{\sum_{q=0}^Q (s-2qd)^2}{\frac{\pi}{4} d} - 1 \right] \right)$$

Finally, the total number of exposed cells (without overcounting those on edges or vertices) is defined as:

$$\langle N_{exposed} \rangle = 2 * n_1 + 2 * n_3 + 2 * n_5$$

After making the substitutions for $n_1 - n_6$ and dividing by two, this can be written as:

$$\langle N_{exposed} \rangle = \left[\frac{64 \sum_{q=0}^Q (s-2qd)^2}{\pi^3 d^2} * P \right] + \left[\frac{64 \sum_{q=0}^Q (s-2qd)^2}{\pi^3 d^2} * P - 2 \frac{\sum_{q=0}^Q (s-2qd)}{\frac{\pi}{4} d} * P \right] + \left[\frac{64 \sum_{q=0}^Q (s-2qd)^2}{\pi^3 d^2} * P - 4 * P \left(\frac{\sum_{q=0}^Q (s-2qd)}{\frac{\pi}{4} d} - 1 \right) \right]$$

Where:

d = cell diameter (μm)

s = side length of identical, idealized cubes (μm)

q = total number of beached layers of cells in the cubical almond particle

Once again, since it is assumed that only exposed cells release their lipid contents, the percentage of lipid released from the idealized cube can be expressed as the ratio of exposed cells to the total number of cells.

$$\text{Lipid release (\%)} = L = \frac{\langle N_{\text{exposed}} \rangle}{\langle N_{\text{total}} \rangle} * 100\%$$

Where:

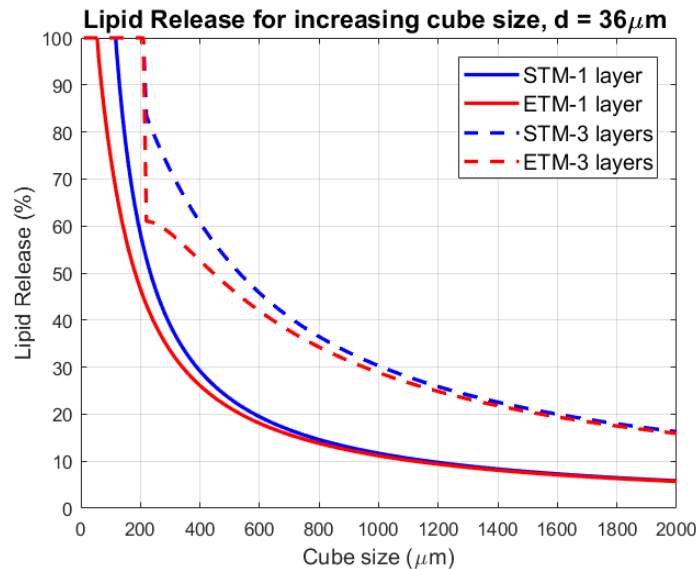
L = lipid release = percentage of lipid release from the almond particle during digestion

$\langle N_{\text{exposed}} \rangle$ = total number of cells that become exposed to sufficient acid to breach their cell walls over the entire course of digestion

$\langle N_{\text{total}} \rangle$ = total number of cells in a cube of size s , defined previously

Grassby, et. al. refer to this model as the Extended Theoretical Model. Once again, the packing density of the spherical cells into the almond cubes cancels out. As in the derivation of the STM, Grassby, et. al. did not consider the contribution from cells beneath the initial surface layer.

Since the STM does not account for the existence of spheres which are shared by multiple facets of the cube, any spheres on the boundary between facets are counted twice, and those on vertices are counted three times, resulting in the STM always predicting a higher number of exposed lipid containing cells for a given cube and cell size, in comparison to the ETM. Thus, the STM always predicts higher lipid release than the ETM for a given cube and cell size. However, the relative significance of this difference between the two models decreases as the size of the cube increases. At a cube size of $1000\mu\text{m}$, cell size of $36\mu\text{m}$, and only cells on the initial surface (one layer) contributing to lipid release, the predictions of the ETM and STM differ by only 4.4%. This is because the number of cells on the bulk, central part of the facets becomes much larger than the number of cells located on the edges and vertices of the cube. This is visualized in the following figure:



It can be seen from the visualization that the STM always predicts higher lipid release than the ETM, for a given cell diameter and number of layers breached. This is because it over-counts the cells on edges and vertices of the almond cube. However, the magnitude of the difference between them decreases as particle size increases, due to the declining relative contribution of lipid from these cells, with respect to cells on the faces of the cube. Also, it can be seen that the lipid release is higher when more layers are breached. This is also intuitive, as these cells are assumed to contribute zero lipid under the original models constructed by Grassby, et. al, but in the new, proposed model are allowed to contribute lipid if the acid has diffused far enough into the particle.

It is important to note a few general points that apply to both the STM and ETM models. First, the release of lipid is dependent only upon the size of cubes, s , the diameter of cells, d , and the number of additional exposed layers, q . Second, the model is not yet set up to contend with a distribution of almond particles, which is the realistic outcome of most processing operations of almonds, as well as mastication of whole almonds²⁵⁻²⁷. This is an opportunity for extending and improving the model.

Model Expansion- Consideration of a Distribution of Particle Sizes

Because mastication of a brittle food results in a distribution of particles, relaxing the assumption in the Grassby model that all particles were of the same size and shape was considered an opportunity for improving the model. This was done by allowing the equation for lipid release to operate on an ensemble of particles of varying sizes, drawn from an arbitrarily defined discrete distribution. In practice, the real distribution of almond particle sizes could be characterized using sizing techniques such as sieving or quantitative imaging. These avenues have been explored by previous researchers to characterize the distribution of particle sizes from fractured almonds^{13,18,28}. The use of a distribution of particle sizes was explored for two cases.

First, a discrete case was examined in which a known number (population) of particles was drawn from a distribution, used as an input to the function for lipid release (STM or ETM) and the overall lipid release calculated empirically. In the second case, an analytical probability mass function (PMF) describing a continuous distribution of particles was used as an input into the lipid release function, and the overall lipid release from the ensemble of particles drawn from the given distribution was derived analytically. First, the discrete case is examined.

Discrete case

For this case, a sample of particles was populated by random sampling from a Gaussian distribution with a desired mean and standard deviation, using the following code:

$$f = \sigma * randn(N) + \mu$$

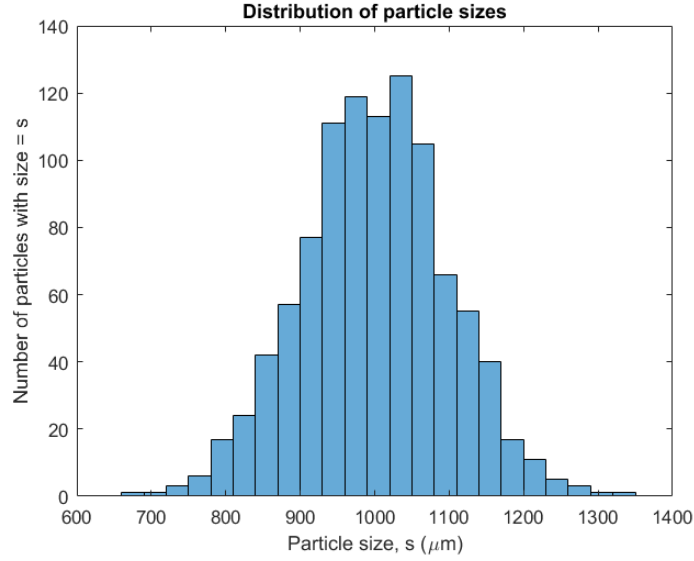
Where:

σ = standard deviation of the particle size distribution

$randn(N)$ = random number generator drawing N samples from a standard normal distribution ($\mu=0$, $\sigma=1$)

μ = mean of the particle size distribution

An example distribution is shown below, for parameters $\sigma = 100 \mu\text{m}$, and $\mu = 1000\mu\text{m}$.



Next, the percentage of lipid released from this ensemble of particles was calculated. This was done by separately calculating the percentage of lipid released from each bin of particles on the histogram, and then evaluating a mass-average of all lipid release percentages to determine the overall lipid release from the ensemble. First, the percentage of lipid released from each bin was calculated. This discretization introduced the approximation that all particles with size ranging from the lower bound of a bin to the upper bound of the same bin were treated as having size equal to that of the center of the bin. This was repeated for each bin on the histogram. An example calculation for bin 1 is shown:

$$ETM: Lipid release (\%) = \frac{1}{2} \left[\frac{64}{\pi^2} \left(\frac{d}{s} \right) - 8 \left(\frac{d}{s} \right)^2 + \frac{4}{3} \pi \left(\frac{d}{s} \right)^3 \right] * 100\%$$

The ETM with only one layer of particles released is shown here for simplicity. Next, a weighting factor was calculated as the mass fraction of particles in each bin divided by the total mass of all particles. An example expression for bin 1 is shown:

$$Weight(s = s_1) = \frac{Mass\ particles\ in\ bin\ s_1}{Mass\ total\ particles}$$

$$Weight(s = s_1) = \frac{\langle N_1 \rangle * V_1 * \rho}{\sum_{i=1}^{i=nbins} \langle N_i \rangle * V_i * \rho}$$

Where:

$\langle N_1 \rangle$ = number of particles in bin 1

V_1 = volume of a single particle in bin 1 = s_1^3

ρ = particle density

i = bin number, from 1 to number of bins on the histogram

$\langle N_i \rangle$ = Number particles in bin i

V_i = Volume of a particle in bin $i = s_i^3$

It was assumed that particle density was constant regardless of particle size, allowing it to be cancelled out. Thus, the mass fraction reduced to a volume fraction exemplified by the following expression for bin 1:

$$Weight(s = s_1) = \frac{\langle N_1 \rangle * s_1^3}{\sum_{i=1}^{nbins} (\langle N_i \rangle * s_i^3)}$$

Finally, the lipid release percentage calculated for each bin was multiplied by its corresponding weighting factor. It was shown above that under the assumption of constant particle density this weighting factor reduces from a mass fraction to a volume fraction. The weighting factor for any particular bin of particles is the same as the ratio of the volume occupied by particles in that bin to the total volume of particles in the population. This final calculation for overall lipid release is shown below:

$$Overall Lipid Release (\%) = \sum_{i=1}^{nbins} L(s_i, d = d_o) * \frac{V_i}{V_{total}}$$

$$Overall Lipid Release (\%) = \sum_{i=1}^{nbins} L(s_i, d = d_o) * \frac{\langle N_i \rangle * s_i^3}{\sum_{i=1}^{nbins} (\langle N_i \rangle * s_i^3)}$$

Where:

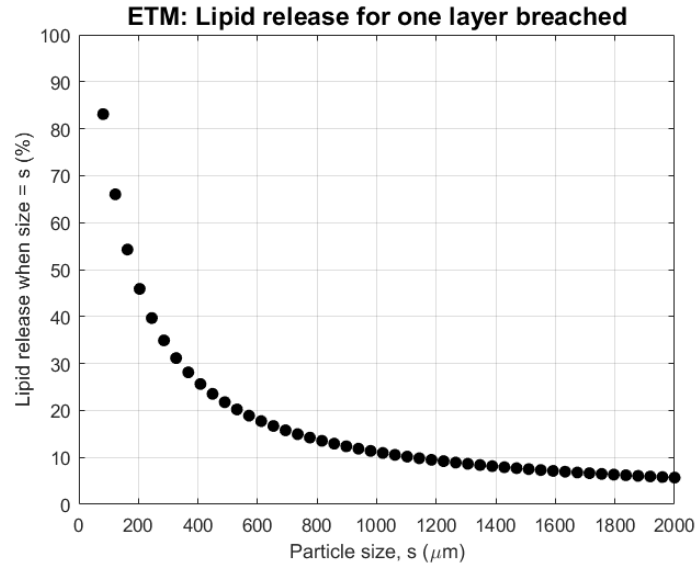
$L(s_i, d = d_o)$ = Lipid release for particle size s , assuming constant cell diameter, d_o

$\langle N_i \rangle$ = number of particles in bin i

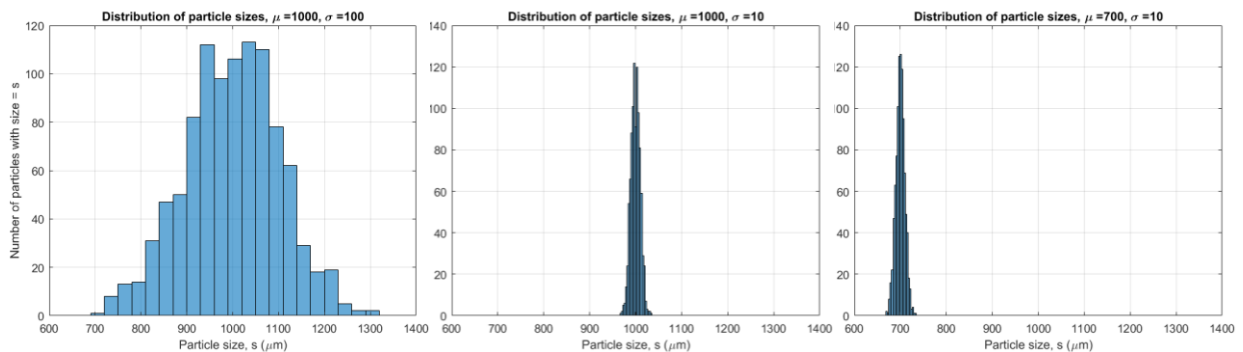
i = bin number, from 1 to number of bins on the histogram

s_i = size of particles in bin i , assuming all particles in a bin (of arbitrary width) have the same size

For each particle size, the ETM can be used to predict a certain endpoint lipid release (expressed as a percentage), given a constant cell diameter and a known number of layers that are breached during digestion. Below, the results are shown for cell diameter, d , of 36 μ m, and only the outer layer of cells being breached.



If all particles in the ensemble are the same size, the total lipid release percentage for the ensemble is equal to the percent lipid release for a single particle. However, in the case that particles in the ensemble have a distribution of sizes, the overall lipid release percentage can still be calculated using the ETM. In this case, the model is used to evaluate the percent lipid release from every particle individually, and then they are weighted using a mass fraction as described above. A few example calculations of overall lipid release for a distribution of particles are shown below:



Left: Overall lipid release for distribution with $\sigma=100 \mu\text{m}$, and $\mu=1000\mu\text{m}$ is 10.98%.
Middle: Overall lipid release for distribution with $\sigma=10 \mu\text{m}$, and $\mu=1000\mu\text{m}$ is 11.16%.
Right: Overall lipid release for distribution with $\sigma=10 \mu\text{m}$, and $\mu=700\mu\text{m}$ 15.64%.

It is noted that the result of 11.16% overall lipid release for the very narrow distribution with mean 1000 μm is in good agreement with the value reported by Grassby, et. al. for the monodisperse sample of particles with the same size ($L = 11.2\%$), as well as for the case when particle size was 700 μm ($L=15.7\%$)³.

The overall lipid release for the distribution with mean particle size of 700 μm was higher than that of the distribution with the same variance but mean of 1000 μm (15.64% vs 11.16%). This is

intuitive because the ratio of the number of surface cells to the number of total cells is higher for smaller particles. This ratio is the same as the scaled surface area to volume ratio. When comparing two samples from Gaussian distributions of equal variance, the sample drawn from the distribution with smaller mean particle size will have a higher release of lipid. In the next section, a continuous distribution of particle sizes will be used as an input to the equation for lipid release.

Continuous case

To generate a continuous distribution for describing particle sizes, a closed form expression for a Gaussian distribution centered on a desired mean and with a desired standard deviation was used:

$$P(s) = \frac{1}{\sqrt{2\pi\sigma^2}} * e^{\left(-\frac{(s-\mu)^2}{2\sigma^2}\right)}$$

Where:

$P(s)$ = probability of particle with size s

σ = standard deviation of particle size (μm)

μ = mean particle size (μm)

s = particle size, continuous variable defined on $[0, \infty)$

Next, the mass average lipid release was evaluated for the continuous distribution of particle sizes represented by $P(s)$:

$$\text{Overall lipid release (\%)} = \frac{\int_{s=0}^{\infty} (L(s, |d) * P(s) * s^3) ds}{\int_{s=0}^{\infty} (P(s) * s^3) ds}$$

Where:

$L(s|d)$ = Lipid release for particle size s , given constant cell diameter, d

$P(s)$ = probability of particle size s

s = particle size, continuous variable defined on $[0, \infty)$

d = constant cell diameter, μm

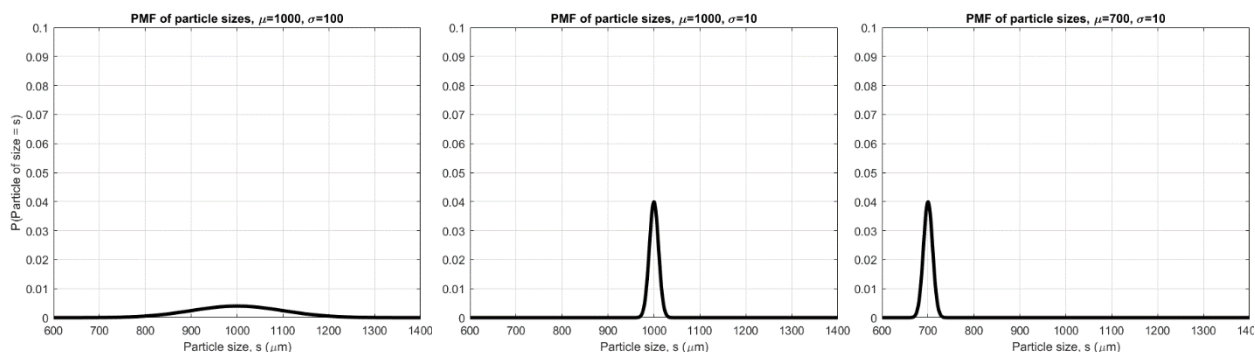
This is anticipated to result in the same mass average lipid release (for a given distribution of particles) as was calculated using the discrete implementation, provided that the population of particles in the discrete case is large enough for the underlying distribution to be reflected by the sample, without any significant influence of stochastic effects. The discrete formula for overall lipid release is restated below:

$$\text{Overall lipid release (\%)} = \sum_{i=1}^{i=nbins} L(s = s_i) * \frac{\langle N_i \rangle * s_i^3}{\sum_{i=1}^{i=nbins} (\langle N_i \rangle * s_i^3)}$$

In the discrete case, the overall lipid release is calculated using the lipid release for a certain particle size multiplied by number of particles in a given range centered on that size, multiplied by their volume, and divided by the total volume of all particles.

In the continuous case, overall lipid release is calculated using the integral of lipid release (as a function of s) multiplied by the probability of a particle at size s , multiplied by the volume of the particle at size s , divided by the integral of all particle probabilities multiplied by their corresponding volumes.

A few example calculations of overall lipid release for a distribution of particles are shown below. This is a re-visitation of the calculations of overall lipid release that were conducted for discrete samples of particles that were generated using the same parameters.



Left: Overall lipid release for distribution with $\sigma=100 \mu\text{m}$, and $\mu=1000\mu\text{m}$ is 10.95%.

Middle: Overall lipid release for distribution with $\sigma=10 \mu\text{m}$, and $\mu=1000\mu\text{m}$ is 11.16%.

Right: Overall lipid release for distribution with $\sigma=10 \mu\text{m}$, and $\mu=700\mu\text{m}$ 15.64%.

These results are in good agreement with those calculated for samples of particles drawn randomly from distributions with the same parameters. They are compared in the following table:

Table 1: Comparison of discrete and continuous consideration of a distribution of almond particles with respect to percent lipid release

Underlying distribution properties	Overall percent lipid release		Percent difference
	Discrete sample	Continuous distribution	
$\mu=1000, \sigma=100$	10.98%	10.95%	0.27%
$\mu=1000, \sigma=10$	11.16%	11.16%	0.00%
$\mu=700, \sigma=10$	15.64%	15.64%	0.00%

In summary, it seems that the discrete distribution and continuous distribution implementations are in good agreement for overall lipid release from arbitrarily defined Gaussian distributions of particle sizes. This leads to another opportunity for model improvement, as it is desirable to quantify the relative change in overall lipid release for changes in the parameters of the particle size distribution such as mean and standard deviation.

Results and Discussion: Solution to the Proposed Model

To solve the diffusion PDE introduced above, the PDEPE function in MATLAB r2017a was utilized. The following parameters were used in the script:

Governing Equation

$$\frac{\partial C}{\partial t} = \frac{-A}{\log(C)} \frac{\partial^2 C}{\partial x^2}$$

BCs:

$$C\left(x\left(\frac{s}{2}\right), t\right) = 10^{-1.8}$$
$$\frac{\partial C}{\partial x} = 0 \text{ at } x = 0$$

IC:

$$C(x, 0) = 10^{-7}$$

Variables

$$C = 1$$
$$f = -A/\log_{10}(u) * DuDr$$
$$s = 0$$
$$u0 = 1e-7$$
$$p1 = u1 - 10^{(-1.8)}$$
$$q1 = 0$$
$$pL = 0$$
$$qL = 1$$

The function c is the multiplier of the derivative on the left-hand side of the equation, which in this case is equal to one. The function f is the forcing function, which in this case is equal to the diffusivity multiplied by the derivative of concentration with respect to distance into cell wall material. The source function is zero, as acid hydrolysis of cell wall material is predicted to be catalyzed by acid, and thus consume a negligible amount. These are shown as part of *pdeAlmondpe*:

```
function [c, f, s] = pdeAlmondpe(r, t, u, DuDr) %definition
    global A
    c = 1; %multiplier of time deriv (on LHS)
    f = A/-log10(u) * DuDr;
    s = 0;
end
```

Next, the initial conditions were provided using a separate function called *pdeAlmondIC*. This function defines the initial value of the acid concentration inside the almond as the value corresponding to neutral pH.

```
function u0 = pdeAlmondIC(r) %Initial conditions
    u0 = 1e-7; %initial almond pH
end
```

Finally, the boundary conditions are provided using a separate function called *pdeAlmondBC*. This function sets the concentration of acid at the boundary of the almond particle to be equal to the concentration of acid in the bulk solution. The interior of the almond particle is set to have a gradient equal to zero due to symmetry.

```
function [p1, q1, p2, q2] = pdeAlmondBC(r1, u1, r1, u1, t) %BC xone uone xL uL
    p1 = u1 - 10^(-1.8); %C at boundary = Cbulk
    q1 = 0; %no dudx term in this BC

    p2 = 0;
    q2 = 1;
end
```

Using this implementation, the model could be solved for concentration of acid in the almond particle at any linear distance from the surface of the particle and at any time on the desired interval of 12 hours. However, the diffusivity which was modeled as dependent on the concentration, still has an unknown coefficient, A . In order to determine an appropriate value for this term, the experimental results of Mandalari, et. al (2008) were used, in which the authors determined that an almond digested in gastric conditions using an *in vitro* system experienced about 5 layers of ablation from its surface in the experimental time interval of 12 hours.

In accordance with the model shown in Figure 5, lipid release from the first 5 layers of almond cells would require hydrolysis of 8 cell walls. This is due to the fact that going from any layer to the next layer requires hydrolysis of two cell walls: the “back facing” cell wall of the already breached layer, and the “outer facing” cell wall of the preceding layer. Furthermore, the outermost layer was assumed to only present one cell wall to break, instead of two, as it is assumed to be ruptured at the onset of digestion due to mastication or other size reduction of the almond particles, in accordance with the original model assumptions. Thus, a method for calculating an appropriate value of A was implemented in MATLAB. Using this approach, a wrapper function for the entire *pdepe* function was created which included the member functions *pdeAlmondpe*, *pdeAlmondBC*, and *pdeAlmondIC*. This function was allowed to accept an input value of A to serve as a guess, and reported the number of cell walls that were breached at the final time point of 12 hours. The function was called on a vector of guesses for A , increasing from very small to larger values with the knowledge that increasing the diffusivity of acid would increase the number of cell wall layers breached in a given time. The process was stopped when a value of A was used that resulted in the breaching of 8 layers. This was executed using a “for” loop, which is shown below.

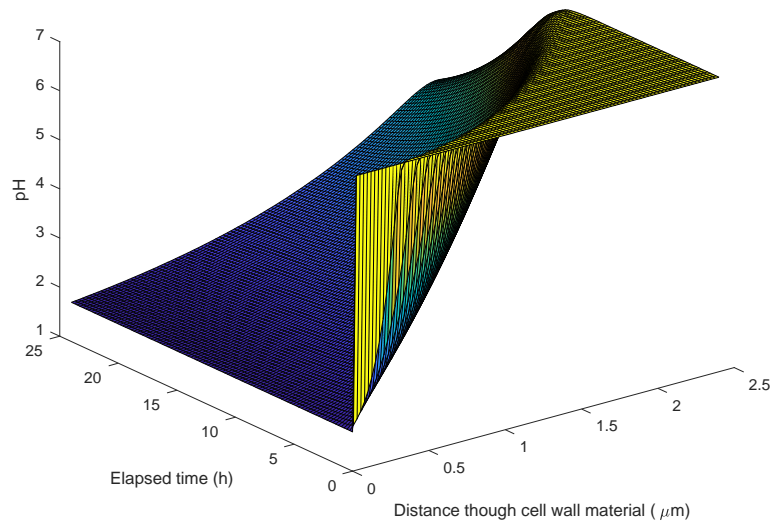
```

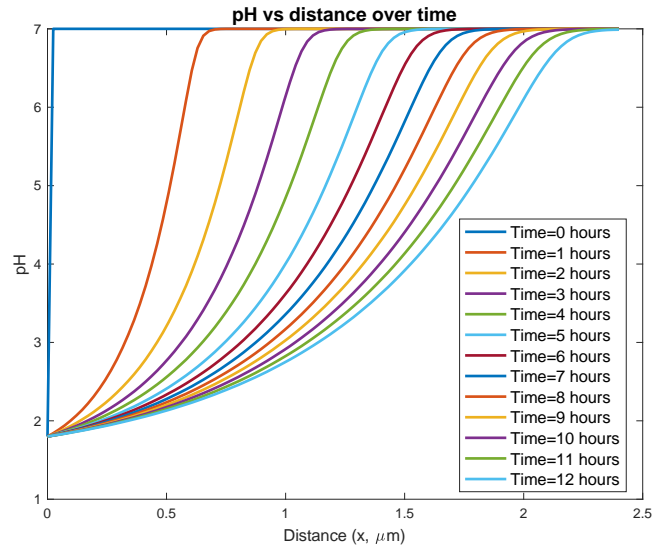
Avalues = linspace(1e-12, 1e-3, 100);
for i=1:1:100
    [~, ~, u, uLast, test_walls] = pdeAlmond(Avalues(i));
    test_walls(i) = test_walls;
    if test_walls >= 8
        winning_Dval = Avalues(i);
        break
    else
    end
end
end

```

The value of A that resulted in 8 cell walls being breached (with the threshold being that the pH gradient reached a value of 3) was found to be $1.01 \cdot 10^{-5}$. Next, the model was solved, this time using this calculated value of A .

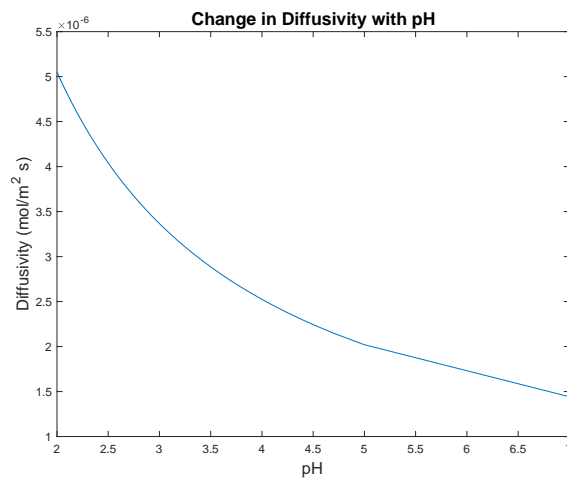
pH in the almond particle vs time and distance



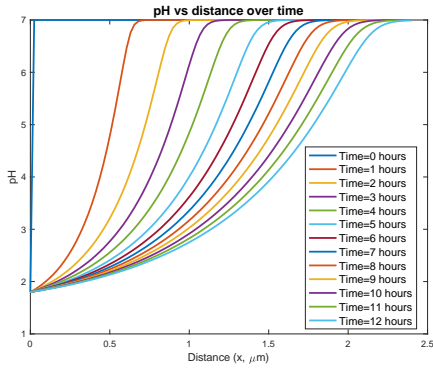


The surface plot and concentration profiles above represent the solution to the partial differential equation. Both plots demonstrate that over time, the pH in the almond approaches the pH in the bulk media. Additionally, the concentration profile becomes less steep over time.

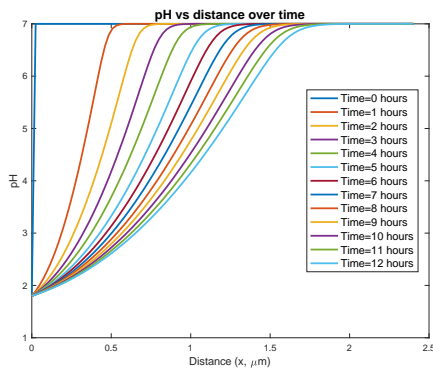
Due to the relationship between H^+ concentration and diffusivity, the figures above show a concentration profile weighted towards lower pH values. This is due to the inverse relationship between pH and diffusivity. See the figure below for a visual depiction of this relationship.



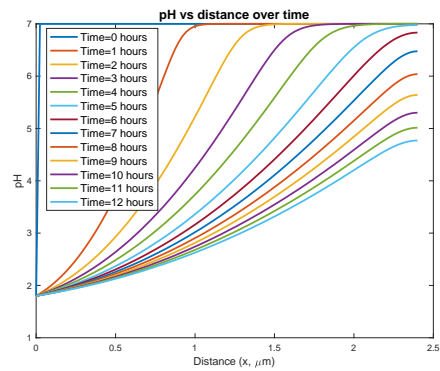
In the figure below, the solution from above is reproduced and compared to the model solutions assuming smaller and higher D values. The smaller constant D value was calculated assuming the D value was equal to the D value at pH 7 in the proposed model, and the larger constant D value was represented by the D value in the proposed model at pH 1.8.



A



B

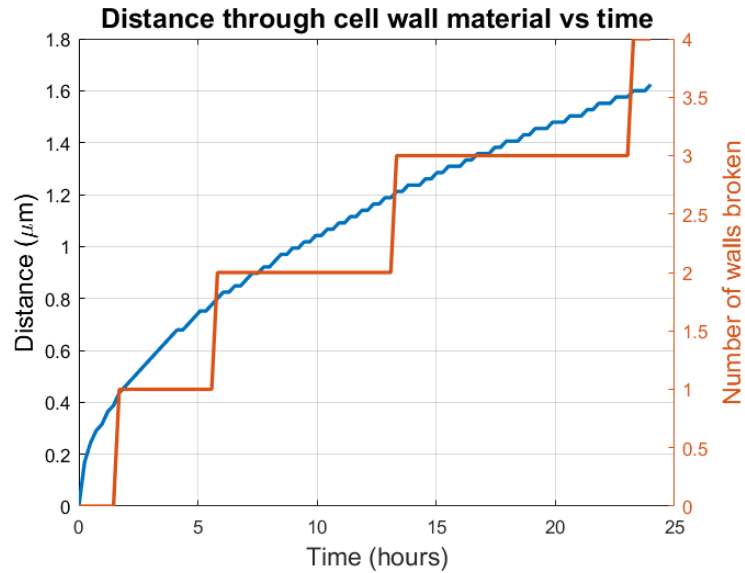


C

Plot A is the reproduced pH vs. distance plot considering a D value changing as a function of concentration. Plot B assumes a constant D value of 1.44×10^{-6} , and Plot C assumes a constant D value of 5.61×10^{-6}

Compared with the concentration profiles assuming a high D value (Plot C), the generated solution to the proposed model (Plot A) does not show significant pH decrease at the edge of the plot, representing a location of $2.5 \mu\text{m}$ into the almond particle. However, the pH at locations closer to the surface is decreased relative to the profile assuming a small D value (Plot B). Thus, the diffusivity is weighted towards lower pH values in this model.

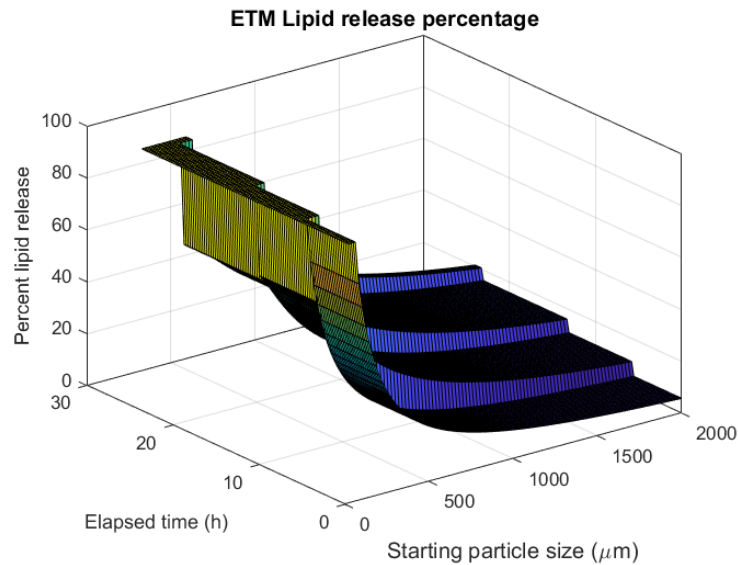
Following the analysis of the A parameter, the effect of progressive hydrolysis of layers of cells from the almond particle was considered using the geometrical model proposed by Grassby, et. al. From solving the diffusion model, the concentration of acid at each distance into the almond particle as a function of time was developed. By setting a threshold of $\text{pH} = 3$ for cell wall breakage, the location of the front where pH is 3 was related to a discrete number of layers that have been breached. This is shown in the following figure.



The distance was divided by the thickness of two cell wall equivalents, $0.4 \mu\text{m}$, and then rounded down to the nearest whole number. The red line on the plot above denotes the result of this manipulation, which is defined as $q(t)$ in the proposed model. This line represents the number of layers beneath the surface layer that have been ruptured at a given time.

The typical residence time for solid foods in the stomach is approximately 4 hours in a healthy individual²⁹. However, longer gastric retention times can be achieved by changing the properties of the food matrix being digested. It has been shown that increasing viscosity and caloric content decreases gastric emptying of solid food³⁰, thus extending the retention time of the food in the stomach. Additionally, particle size has been shown to be directly related to gastric retention time—smaller particles exit the stomach faster than larger particles³¹. If, in this case, if the almond particles are held in the gastric environment for over 6 hours, the model predicts that a second inner layer would rupture and therefore release lipid into the lumen.

To provide more insight into the lipid release itself, this result was incorporated into the geometric model for lipid release. In a previous figure the results were shown for one layer of lipid release as well as three layers, but here, the time dependency of additional layers was considered. The diffusion model allows for the calculation of the number of additional layers which are breached as a function of time, and the modified Grassby model allows consideration of extra layers from the cubic almond particle.



When the cube size approaches the size of the almond cell, the contribution of lipid from exposed cells (the numerator of the model) can become artificially large, as the packing density cancelling is no longer relevant. This was noticed by the previous authors Grassby, et. al (2014) and results in a predicted value of lipid release greater than 100% when particle size is small. To deal with this issue the lipid release was constrained to 100%.

As shown in the above figure, the consideration of additional layers occurs as a step function. This is because the lipid contribution from a given layer was either fully assessed if it has been breached, or not assessed at all if it has not been breached. As stated previously, the condition for a layer being breached is that the pH reaches a value of 3 at that depth inside the particle. Since the number of layers that were breached was assessed as a step function, the resulting time dependent lipid release took on the same appearance.

The model demonstrates that as time increases, the lipid release from a given sized particle is predicted to increase. This is because the particle has additional layers worn away. It can also be seen that for a given digestion time, for instance 12 hours, higher lipid release is achieved from smaller particles. It is important to note, however, that this graph does not consider a true distribution of particle sizes.

The following table provides the lipid release for some selected particle size distributions. The solutions represented in the table are those of the STM, and the release was calculated for a discrete distribution of almond particle sizes.

Table 2: Effect of particle size distribution parameters on lipid release

Mean (μm)	Standard Deviation (μm)	Lipid Release from Outer Surface (Percent)	Lipid Release Including One Inner Layer (Percent)	Lipid Release Including Two Inner Layers (Percent)
1000	100	11.5	21.4	29.8
1000	200	10.8	20.2	28.2
1000	100	11.5	21.4	29.8
2000	100	5.82	11.2	16.2
2000	100	5.82	11.2	16.2
2000	200	5.73	11.1	16.0
		0 - 1.7 hours	1.7 - 5.8 hours	5.8 - 13.3 hours

As shown in the table above, a broader particle size distribution results in a lowered amount of lipid release. This is due to the fact that larger particles have more mass, and therefore the percent lipid release, which is related to the original mass of lipid in the sample, decreases. However, the table also shows that the lipid release for a normally distributed set of particles is influenced to a greater extent by the mean of the distribution than by the variance.

The degree to which the lipid release changes as a function of mean particle size can be expressed for single particle sizes and for a distribution of particle sizes by the modified STM and ETM models presented in this report. However, there is opportunity for additional study of the system by quantifying the rate of change of lipid release with the mean of any distribution. This is discussed in greater detail in a later section.

Potential Expansion to the Proposed Model: Rate of Change of Lipid Release as a Function of Mean Particle Size

This can be expressed as the partial derivatives of the continuous form equation for overall lipid release with respect to μ and σ , as shown below:

$$\frac{\partial L_{overall}}{\partial \mu} = \frac{\partial \left\{ \frac{\int_{s=0}^{\infty} (L(s|d) * P(s) * s^3) ds}{\int_{s=0}^{\infty} (P(s) * s^3) ds} \right\}}{\partial \mu}$$

Where:

$L(s|d) = \frac{1}{2} * \left(\frac{64}{\pi^2} * \frac{d}{s} \right) * 100\%$ = Lipid release as predicted by STM, given a known, constant cell diameter and only one layer of cells being breached.

d = constant cell diameter, μm

$P(s) = \frac{1}{\sqrt{2\pi\sigma^2}} * e^{\left(\frac{-(s-\mu)^2}{2\sigma^2} \right)}$ = probability of particle size s

σ = standard deviation of particle size (μm)

μ = mean particle size (μm)

s = particle size, continuous variable defined on $[0, \infty)$

In this case, the STM was used for simplicity.

$$\frac{\partial L_{overall}}{\partial \mu} = \frac{\partial \left\{ \frac{\int_{s=0}^{\infty} \left(\frac{1}{2} * \left(\frac{64}{\pi^2} * \frac{d}{s_1} \right) * 100\% \right) \left(\frac{1}{\sqrt{2\pi\sigma^2}} * e^{\left(\frac{-(s-\mu)^2}{2\sigma^2} \right)} \right) s^3 ds}{\int_{s=0}^{\infty} \left(\frac{1}{\sqrt{2\pi\sigma^2}} * e^{\left(\frac{-(s-\mu)^2}{2\sigma^2} \right)} \right) * s^3 ds} \right\}}{\partial \mu}$$

This can be algebraically simplified to:

$$\frac{\partial L_{overall}}{\partial \mu} = \left(\frac{3200d}{\pi^2} \right) \frac{\partial \left\{ \frac{\int_{s=0}^{\infty} \left(s^2 e^{\left(\frac{-(s-\mu)^2}{2\sigma^2} \right)} \right) ds}{\int_{s=0}^{\infty} \left(s^3 e^{\left(\frac{-(s-\mu)^2}{2\sigma^2} \right)} \right) ds} \right\}}{\partial \mu}$$

This derivative was solved as a symbolic expression using MATLAB, but it should be pursued in a more understandable analytical form as part of the future work. It is hypothesized that the derivative of overall lipid release with respect to the mean of the distribution of particles used as an input will be negative, as the geometrical model that was implemented allows for higher percent lipid release from smaller particles due to their higher surface area to volume ratios than large particles. This means that as the mean size of the particles in the distribution increases, the percentage of lipid released should go down. This is supported by the results from the example calculations.

Another interesting facet of this would be to see if the rate of change of overall lipid release with respect to the mean size of a particle in the input distribution is the same regardless of the specific input distribution. For instance, masticated particles often have a bimodal distribution²⁶, whereas particles from a grinding operation are roughly normally distributed. Using the previous steps, it could be determined whether or not the rate of change of lipid release with respect to mean particle size would be the same for foods whose distribution of particles is described by different models (Gaussian, bimodal, heavy-tailed models, ect). This work could help guide food processing operations and inform decisions for functional foods. For instance, if it was desired to conduct a size reduction operation on almonds for the purpose of creating a food with rapid and total release of lipid during digestion, this work could help optimize the processing operation by revealing the size threshold at which all of the lipid would be released and thus prevent overgrinding, an important consideration for manufacturers due to costs associated with operating size reduction equipment. Alternatively, this model might be used to help guide selection of specific equipment to create distributions of particle sizes with desired characteristics.

Another modeling step that should be pursued is the consideration of the derivative of lipid release with respect to the shape or spread parameters of the distribution of particles. For the normal distribution, this would be done by evaluating the derivative of lipid release with respect to the variance of the distribution.

Since real world size reduction operations such as milling, grinding, and mastication result in a distribution of particle sizes, this knowledge could be useful for enabling prediction of the effect of changing the spread of the distribution of particles on the rate of lipid release from them when they enter human digestion. Processing equipment can be used to predictably change the spread of the distribution of particles. For instance, a mixture of particles can be sieved, and the retentate recycled back into the size reduction step to further decrease size. Alternatively, the permeate can be discarded to remove particles with size beneath a desired threshold. With the ability to predict lipid release as function of particle distribution parameters, perhaps these two size fractions could even be used for two different food products with different targeted release rates of lipid.

Model Validation and Limitations

The results of lipid release from an almond cube with various particle sizes obtained from the model were compared to the experimental results of processed almonds with similar particle sizes and same digestion times, as shown in table below. It should be noted that for the 2 and 3 hour digestion times referenced below, the proposed model predicts the release of lipid from one inner layer, in addition to the surface layer. The results suggest that upon the same gastric digestion time (2 h), the lipid release (%) from almond cubes increases significantly when the particle size of almond cubes decreases: for an average size of 2000 μm as demonstrated earlier, the model predicted that 2 layers of lipid cells breach after 2h of gastric acid diffusion into the almond matrix, and 11.01% of lipid is released. When the average size is reduced to 200 μm , the number of layers breached by the acid diffusion predicted by the model was still 2, but the lipid release increased to 61.69%. This is reasonable as the surface area of the processed almonds gets larger when the individual almond cube gets smaller. Therefore, although the same number of lipid cell layers were breached, the total number of lipid cells that have been breached was greater in almond cubes with smaller size than in cubes with large size.

Another interesting result to notice is that when the particle size of almond cubes is constant (e.g. 2000 μm), same result of lipid release (11.01%) was predicted by the model for the GD time of 2h and 3h respectively. This is due to the fact that the number of breached layers was still 2 after 3 h of acid diffusion, thus the number of total lipid cells been breached was the same to that of 2h of acid diffusion. This corresponds well to the experimental results reported by Mandalari et al (2008) and Grassby et al (2014): the lipid release from almond cubes with an average size of 2000 μm after 2h of in vitro gastric digestion was $9.7 \pm 0.38\%$, which is very close to the lipid release of the same sized almond cubes after 3h of in vitro digestion ($9.9 \pm 0.71\%$). These two experimental results are also close to the predicted results by the model (11.01%).

Table 3. Comparison of modeled lipid release with experimental results from previous studies

Processed type	Particle size* (μm)	In vitro GD** time (h)	Model predictions		Experimental results	Literature source
			Number of breached layers	Lipid release (%)	Lipid release (%)	
Natural almond (cut cubes)	~2000	2	2	11.01	7.6 ± 0.18	Mandalari et al (2008)
Blanched almond (cut cubes)	~2000	2	2	11.01	9.7 ± 0.38	
Finely ground almonds	~200	2	2	61.69	31.1 ± 0.25	
Natural almond (cut cubes)	~2000	3	2	11.01	9.9 ± 0.71	Grassby et al (2014)
Finely-ground flour	~250	3	2	57.42	39.3 ± 0.18	

*: the approximated values for particle sizes, either as the average or the mean.

** : GD refers to gastric digestion.

However, it is also noticed that for almond particles with small sizes, the predicted lipid release results do not match well with the experimental results obtained from previous studies. For instance, for finely ground almonds with an average particle size of 200 μm , the predicted lipid release after 2h of acid diffusion was 61.69%, which is much higher than the lipid release of $31.1 \pm 0.25\%$ reported by Mandalari et al (2008) through in vitro experiments. In addition, for finely ground flour with an average particle size of 250 μm , the predicted lipid release after 3h of acid diffusion by the model was 57.42%, which is much higher than the lipid release of $39.3 \pm 0.18\%$ reported by Grassby et al (2014) through in vitro experiments.

These inconsistent results indicate that the model has limitations on predicting lipid release from almonds with smaller particle sizes, possibly because the particle size distribution of processed almonds was not able to be considered in the model due to the limited amount of information provided in the literature references above. Generally speaking, for almonds with smaller average particle size e.g. finely ground powder and almond butter, the particle size distribution can vary significantly, which can affect the model predictions to a great extent if considered. To resolve this issue, a further improvement would be to obtain the detailed particle size distribution by experiments and implement it into the model.

Another limitation of the model is the assumption that all the lipid within a cell would be released simultaneously when the cell wall has been breached by the acid. In real cases, the lipid may be released very slowly and not all the lipid within one cell needs to be released, even if the cell wall has been weakened or breached by acid diffusion. Therefore, this ideal assumption would lead to a higher prediction of lipid release than the actual results from experiments, as discussed above. To solve for this limitation, better knowledge of how lipid is released after the cell wall has been breached would help to refine the model.

Conclusions

Lipid release from almond particles is relevant in multiple ways to health-conscious individuals. In this report, acid diffusion into almond particles during gastric digestion was modeled and coupled with an existing model of lipid release from almond cells as a function of the position of the cells on the almond particle. The pre-existing model considered lipid release from only surface cells, while the expanded model presented in this report considers the potential for increased lipid release from internal cells. It was determined that over the course of a 4 to 6 hour digestion, one to two additional layers of cells in a given almond particle release lipid into the lumen, increasing metabolizable energy intake and post-prandial lipemia. The predicted results from the proposed model were compared with results found in the literature and it was shown that some predicted results agree well with literature values, while some results point out limitations of the model. Future expansions to the proposed model include performing time-dependent *in vitro* and *in vivo* digestions to validate the model against robust experimental data as well as attempting to visualize the lipid release from the almond matrix over time to better understand the mechanism driving the process.

References

1. Parada, J. & Aguilera, J. M. Food microstructure affects the bioavailability of several nutrients. *J. Food Sci.* **72**, 21–32 (2007).
2. Grundy, M. M. L., Lapsley, K. & Ellis, P. R. A review of the impact of processing on nutrient bioaccessibility and digestion of almonds. *Int. J. Food Sci. Technol.* **51**, 1937–1946 (2016).
3. Grassby, T. *et al.* Modelling of nutrient bioaccessibility in almond seeds based on the fracture properties of their cell walls. *Food Funct.* **5**, 3096–3106 (2014).
4. Bornhorst, G. M., Gouseti, O., Wickham, M. S. J. & Bakalis, S. Engineering Digestion: Multiscale Processes of Food Digestion. *J. Food Sci.* **81**, R534–R543 (2016).
5. Ansar, S., Koska, J. & Reaven, P. Postprandial hyperlipidemia, endothelial dysfunction and cardiovascular risk: focus on incretins. *Cardiovasc. Diabetol.* **10**, 61 (2011).
6. Hyson, D., Rutledge, J. C. & Berglund, L. Postprandial lipemia and cardiovascular disease. *Curr. Atheroscler. Rep.* **5**, 437–444 (2003).
7. Karpe, F. Postprandial lipoprotein metabolism and atherosclerosis. *J. Intern. Med.* **246**, 341–355 (1999).
8. Nakamura, K., Miyoshi, T., Yunoki, K. & Ito, H. Postprandial hyperlipidemia as a potential residual risk factor. *J. Cardiol.* **67**, 335–339 (2016).
9. California, A. B. of. Almond Almanac 2015. (2015).
10. Grundy, M. M. L. *et al.* The role of plant cell wall encapsulation and porosity in regulating lipolysis during the digestion of almond seeds. *Food Funct.* **7**, 69–78 (2016).
11. *National Nutrient Database for Standard Reference Release 28.* (2016).
12. Yada, S., Lapsley, K. & Huang, G. A review of composition studies of cultivated almonds: Macronutrients and micronutrients. *J. Food Compos. Anal.* **24**, 469–480 (2011).
13. Gebauer, S. K., Novotny, J. A., Bornhorst, G. M. & Baer, D. J. Food processing and structure impact the metabolizable energy of almonds. *Food Funct.* **7**, 4231–4238 (2016).
14. Novotny, J. A., Gebauer, S. K. & Baer, D. J. Discrepancy between the Atwater factor predicted and empirically measured energy values of almonds in human diets. *Am. J. Clin. Nutr.* **96**, 296–301 (2012).
15. Mandalari, G. *et al.* The effects of processing and mastication on almond lipid bioaccessibility using novel methods of in vitro digestion modelling and micro-structural analysis. *Br. J. Nutr.* **112**, 1521–1529 (2014).
16. Berry, S. E. E. *et al.* Manipulation of lipid bioaccessibility of almond seeds influences postprandial lipemia in healthy human subjects. *Am. J. Clin. Nutr.* **88**, 922–929 (2008).
17. Tamura, M., Okazaki, Y., Kumagai, C. & Ogawa, Y. The importance of an oral digestion step in evaluating simulated in vitro digestibility of starch from cooked rice grain. *Food*

- Res. Int.* **94**, 6–12 (2017).
18. Bornhorst, G. M. & Singh, P. R. Gastric digestion in vivo and in vitro: how the structural aspects of food influence the digestion process. *Annu. Rev. Food Sci. Technol.* **5**, 111–32 (2014).
 19. Grundy, M. M. L., Wilde, P. J., Butterworth, P. J., Gray, R. & Ellis, P. R. Impact of cell wall encapsulation of almonds on in vitro duodenal lipolysis. *Food Chem.* **185**, 405–412 (2015).
 20. Mandalari, G. *et al.* Release of protein, lipid, and vitamin E from almond seeds during digestion. *J. Agric. Food Chem.* **56**, 3409–3416 (2008).
 21. Grundy, M. M. L. *et al.* Effect of mastication on lipid bioaccessibility of almonds in a randomized human study and its implications for digestion kinetics, metabolizable energy, and postprandial lipemia. *Am. J. Clin. Nutr.* **101**, 25–33 (2015).
 22. Selvan, A. *et al.* Molecular dynamics simulations of human and dog gastric lipases: Insights into domain movements. *FEBS Lett.* **584**, 4599–4605 (2010).
 23. Peters, G. H., van Aalten, D. M., Edholm, O., Toxvaerd, S. & Bywater, R. Dynamics of proteins in different solvent systems: analysis of essential motion in lipases. *Biophys. J.* **71**, 2245–2255 (1996).
 24. Ellis, P. R. *et al.* Role of cell walls in the bioaccessibility of lipids in almond seeds. *Am. J. Clin. Nutr.* **80**, 604–613 (2004).
 25. Chen, J. Food oral processing-A review. *Food Hydrocoll.* **23**, 1–25 (2009).
 26. Hoebler, C., Devaux, M. F., Karinthe, A., Belleville, C. & Barry, J. L. Particle size of solid food after human mastication and in vitro simulation of oral breakdown. *Int. J. Food Sci. Nutr.* **51**, 353–366 (2000).
 27. Salles, C. *et al.* Development of a chewing simulator for food breakdown and the analysis of in vitro flavor compound release in a mouth environment. *J. Food Eng.* **82**, 189–198 (2007).
 28. Varela, P., Aguilera, J. M. & Fiszman, S. Quantification of fracture properties and microstructural features of roasted Marcona almonds by image analysis. *LWT - Food Sci. Technol.* **41**, 10–17 (2008).
 29. Minekus, M. *et al.* A standardised static in vitro digestion method suitable for food - an international consensus. *Food Funct.* **5**, 1113–24 (2014).
 30. Marciani, L. *et al.* Effect of meal viscosity and nutrients on satiety, intragastric dilution, and emptying assessed by MRI. *Am. J. Physiol. Gastrointest. Liver Physiol.* **280**, G1227–G1233 (2001).
 31. Urbain, J. L. C. *et al.* The two-component stomach: effects of meal particle size on fundal and antral emptying. *Eur. J. Nucl. Med.* **15**, 254–259 (1989).

Appendix A: Derivation of original Grassby Model-Simple Theoretical Model

In the next section, the derivation will be provided for the original model developed by Grassby et al³ to predict the lipid release from an almond particle as a function of particle size. This original model differs from the expanded version presented in this project as it does not consider the additional surface area contributed to particles from cells beneath those initially on the outermost layer of the particles. This contribution was accounted for in the model development of this project by considering acid diffusion into the particle.

Grassby, et. al. considered the masticated almond to consist of identical, cubical particles. Another assumption made by Grassby, et. al. was that all lipid from a cell on the boundary of the cube is released during digestion, and no lipid from cells in the interior of the cube is released.

The next step in the development of the model was expressing the mass of lipid in an almond sample as function of the mass of the almond sample in grams and the percentage by weight of lipid in almond cotyledon cells (edible almond kernel tissue). The almond sample in this case would consist of a certain mass of almond consumed as part of a meal.

$$\text{Mass of lipid in almond sample} = m L_w$$

Where:

m = mass of almond sample (g)

L_w= percentage of lipid in almond cells, by weight

Next, the number of idealized cubes in an almond sample was expressed as the mass ratio of the entire sample divided by the mass of a single cube:

$$\text{Number of cubes in almond sample} = \frac{m}{s^3 \rho}$$

Where:

m = mass of almond sample (g)

s³ = volume of a cube (μm³)

ρ = density of almond tissue (g/cm³)

Then, the mass of lipid in a single idealized cube of almond tissue was expressed as the product of the percentage of lipid in almond tissue by weight, the size of a cube, and the density of almond tissue.

$$\text{Mass of lipid in cube} = L_w s^3 \rho$$

Where:

L_w= percentage of lipid in almond cells, by weight

s³ = volume of a cube (μm³)

ρ = density of almond tissue (g/cm³)

Finally, the average number of cells in an almond cube was expressed by a volume ratio: the ratio of an almond cube to the volume of an idealized spherical almond cell, times a packing density of spherical cells into the cubical particle.

$$\text{Average number of cells in a cube} = \langle N_{total} \rangle = \frac{s^3}{\frac{4}{3}\pi\left(\frac{d}{2}\right)^3} P$$

Where:

s^3 = side length of a cube (μm^3)

d = diameter of an almond cell (μm)

P = packing density of almond cells into the cube

The total number of exposed cells on a certain cube of almond tissue was expressed as the sum of the number of exposed cells on each individual face of the cube

$$\langle N_{exposed} \rangle = n_1 + n_2 + n_3 + n_4 + n_5 + n_6$$

Where:

$\langle N_{exposed} \rangle$ = number of exposed cells on an entire cube of almond tissue

$n_1 \dots n_6$ = number of exposed cells on each surface of the cube 1-6

Next, the number of exposed cells on a face of the cube was expressed as an area fraction: the area of the face of the cube divided by the area of a idealized spherical cell, but expressed in 2D:

$$n_1 = \dots = n_6 = \frac{s^2}{\text{Area}_{cell}} * P$$

Where:

$n_1 \dots n_6$ = number of exposed cells on each surface of the cube 1-6

s^2 = area of a face of the cube (μm^2)

Area_{cell} = area of a cell with 2D profile diameter d'

P = packing density of almond cells into the cube

The profile diameter of a cell (d') was used instead of its real diameter (d), as the cell diameters were measured using light microscopy, which was a two-dimensional approximation. This is because using light microscopy the researchers were able to measure the area of planar slices of cells, which were actually three-dimensional spheres. The profile diameter was converted to the real diameter using the following expression:

$$d = \frac{4}{\pi} d'$$

Where:

d = real diameter of a cell

d' = two-dimensional measured diameter (profile diameter) of the cell

The linear conversion between profile diameter and real cell diameter was developed by Weibel.

The area of a cell with two-dimensional profile diameter d' was thus:

$$Area_{cell} = \frac{\pi}{4} d'^2$$

Where:

d' = measured profile diameter of cell = $\frac{\pi}{4} d$

$$Area_{cell} = \frac{\pi}{4} \left(\frac{\pi}{4} d \right)^2$$

$$Area_{cell} = \frac{\pi}{4} \left(\frac{\pi^2 d^2}{16} \right)$$

$$Area_{cell} = \frac{\pi^3 d^2}{64}$$

Returning to the equation for the number of exposed cells on a given face of the cube:

$$n_1 = \dots = n_6 = \frac{s^2}{Area_{cell}} * P$$

$$n_1 = \dots = n_6 = \frac{s^2}{\frac{\pi^3 d^2}{64}} * P$$

$$n_1 = \dots = n_6 = \frac{64s^2}{\pi^3 d^2} * P$$

Finally, the total number of exposed cells on a cube was six times the number of the exposed cells on a single face:

$$\langle N_{exposed} \rangle = \frac{6 * 64s^2}{\pi^3 d^2} * P$$

$$\langle N_{exposed} \rangle = \frac{384s^2}{\pi^3 d^2} * P$$

Since it was assumed that only the exposed cells released lipid during digestion, the percentage of lipid released could be expressed as the ratio of the number of exposed cells to the total number of cells in the cube.

$$\text{Lipid release (\%)} = \frac{\langle N_{\text{exposed}} \rangle}{\langle N_{\text{total}} \rangle} * 100\%$$

Where:

$\langle N_{\text{exposed}} \rangle$ = number of exposed cells on a cube, defined previously

$\langle N_{\text{total}} \rangle$ = total number of cells in the cube, defined previously

$$\text{Lipid release (\%)} = \frac{\left(\frac{384s^2}{\pi^3 d^2} * P \right)}{\left(\frac{s^3}{\frac{4}{3}\pi \left(\frac{d}{2}\right)^3} * P \right)} * 100\%$$

$$\text{Lipid release (\%)} = \frac{64}{\pi^2} * \frac{d}{s} * 100\%$$

Finally, the ratio is divided by two, due to the fact that cells fractured in a breakage event (resulting in the formation of the idealized cubes) should not be counted twice.

Thus, the final equation is stated:

$$\text{STM: Lipid release (\%)} = \frac{1}{2} * \left(\frac{64}{\pi^2} * \frac{d}{s} \right) * 100\%$$

This results in a model for the percentage of lipid release from a single almond cube of size s , comprised of identical cells of diameter d . An interesting consequence of expressing the lipid release from the cube in terms of the percentage of total lipid in the cube instead of in absolute terms is that the packing density of the spherical cells in the cube cancels out. Since it was assumed that the masticated almond fractures into an ensemble of identical particles (all are idealized as cubes of side length s), the percentage of lipid release from one cube is the same as the percentage of lipid released from all of the cubes.

However, an assumption of the above model was that the total number of exposed cells on the cube was equal to six times the number of exposed cells on a single face. There is a problem with this assumption, which is that there are some cells which are shared by more than one face. Cells on the edges of the cube (shared by two adjacent faces) are counted twice. Cells on the corners (where three faces intersect) are counted three times. This means that the above model for lipid release will always overestimate the lipid release, by counting some cells as exposed more than once. This simple model was named the Simple Theoretical Model (STM) by Grassby, et. al.

Appendix B: Derivation of original Grassby model-Extended Theoretical Model

The same authors offered an improvement to the STM by preventing cells from being counted more than one time. This was done by defining the number of exposed cells on two opposite faces of the cube (called faces 1 and 2). Since these faces are assumed to share no cells with each other, the number of exposed cells on them is expressed in the same way as it was in the development of the STM:

$$n_1 = n_2 = \left(\frac{64s^2}{\pi^3 d^2} * P \right)$$

Next, the number of exposed cells on two more faces are defined. These faces share cells on two sides with the previously defined faces, n_1 and n_2 . Thus, they have slightly less cells.

$$n_3 = n_4 = \left(n_1 - 2 \left[\frac{s}{\frac{\pi}{4} d} * P \right] \right)$$

Finally, the number of cells on the final faces, n_5 and n_6 , were defined. These faces share cells on all four sides with previously defined faces, n_1 -4.

$$n_5 = n_6 = \left(n_1 - 4P \left[\frac{s}{\frac{\pi}{4} d} - 1 \right] \right)$$

Finally, the total number of exposed cells (without overcounting) is defined as:

$$\langle N_{exposed} \rangle = 2 * n_1 + 2 * n_3 + 2 * n_5$$

Which can be algebraically simplified to:

$$\langle N_{exposed} \rangle = \frac{384P}{\pi^3} * \left(\frac{d}{s} \right)^2 - \frac{48P}{\pi} * \left(\frac{d}{s} \right) + 8P$$

Once again, since it is assumed that only exposed cells release their lipid contents, the percentage of lipid released from the idealized cube can be expressed as the ratio of exposed cells to the total number of cells.

$$Lipid\ release\ (\%) = \frac{\langle N_{exposed} \rangle}{\langle N_{total} \rangle} * 100\%$$

$$\text{Lipid release (\%)} = \frac{\left(\frac{384P}{\pi^3} * \left(\frac{s}{d} \right)^2 - \frac{48P}{\pi} * \left(\frac{s}{d} \right) + 8P \right)}{\left(\frac{s^3}{\frac{4}{3}\pi \left(\frac{d}{2} \right)^3} * P \right)} * 100\%$$

$$\text{ETM: Lipid release (\%)} = \frac{1}{2} \left[\frac{64}{\pi^2} \left(\frac{d}{s} \right) - 8 \left(\frac{d}{s} \right)^2 + \frac{4}{3} \pi \left(\frac{d}{s} \right)^3 \right] * 100\%$$

Where:

Lipid release % = Percentage of lipid release from ensemble of almond particles after a “unit” digestion

d = cell diameter (um)

s = side length of identical, idealized cubes (μm)

Grassby, et. al. refer to this model as the Extended Theoretical Model. Once again, the packing density of the spherical cells into the almond cubes cancels out, and the expression is multiplied by a factor of ½ in order to avoid counting fractured cells twice.